ELSEVIER

International Journal of Mass Spectrometry 203 (2000) 127–142

International Journal of Mass Spectrometry

Gas-phase californium ion chemistry

John K. Gibson*, Richard G. Haire

Chemical and Analytical Sciences Division, Oak Ridge National Laboratory, Oak Ridge, TN 37831-6375, USA

Received 11 May 2000; accepted 24 July 2000

Abstract

The gas-phase chemistry of Cf^+ was examined, this now being the heaviest element with which such studies have been performed. The emphasis was on the efficiency of dehydrogenation of alkenes by naked Cf^+; direct comparison was made between the reactivities of Cf^+ and those of Cm^+, Pr^+, and Tm^+. The results with alkenes indicated that Cf^+ is inefficient at C–H bond activation, in accord with a standard mechanistic model, and the reported electronic structure and predicted energy levels for Cf^+. No participation of the quasivalence 5*f* electrons of Cf^+ was indicated, and essentially lanthanidelike behavior was manifested. Other types of reactions were studied, including those of Cf^+ with butryonitrile, butylamine, ethanedithiol, dimethylether, and perfluorocarbons. Several new Cf complex ions were identified, and novel aspects of Cf^+ chemistry were assessed. (Int J Mass Spectrom 203 (2000) 127–142) © 2000 Elsevier Science B.V.

Keywords: Californium; Actinides; Lanthanides; Metal ion chemistry

1. Introduction

The study of gas-phase reactions of naked and ligated metal ions with various reactants has developed into an effective approach for examining fundamental aspects of transition metal chemistry, particularly gas-phase organometallic chemistry [1,2]. Although prudence must be exercised in relating the behavior of free gas-phase metal ions to that of metal species in solution or the solid state, a revealing correspondence can often be established which enables prediction and illumination of key aspects of condensed phase chemistry [3].

Gas-phase studies are particularly well-suited to examining radioactive and scarce metals such as the transuranium actinides. Although a variety of ingenious microscale and tracer techniques have been developed to assess important features of transuranium chemistry [4], the application of these approaches becomes increasingly challenging upon progressing across the series; accordingly, it has often been impractical to investigate many elementary aspects of condensed phase chemistry for the transplutonium elements [5]. Even when compounds of radioactive nuclides can be prepared, self-radiation damage frequently precludes sustained maintenance of structural and chemical integrity for effective characterization by traditional techniques [6].

With the primary goal of enhancing the understanding of transuranic actinide chemistry, a laser ablation time-of-flight technique, laser ablation with prompt reaction and detection (LAPRD), is being applied in our laboratory for the investigation of

*Corresponding author. E-mail: gibsonjk@ornl.gov

PII S1387-3806(00)00294-3

gas-phase chemistries of radioactive actinide (An) positive ions, particularly An^+ and AnO^+ [7]. The LAPRD technique differs from gas-phase metal ion chemistry studies performed in Fourier transform ion cyclotron resonance-mass spectrometry (FTICR-MS) instruments, particularly with regard to the relative reaction timescales: typically 10–100 μs for LAPRD vs. 0.01–1 s for FTICR-MS [8]. The LAPRD technique was employed to investigate the gas-phase chemistries of several lanthanide ions, Ln^+ [7]; concurrence with relative reactivities derived from FTICR-MS studies [9–11] has confirmed the utility of LAPRD in deriving accurate relative metal ion reactivities, despite the short time scale, occurrence of relatively few ion–molecule collisions, and the potential role of electronically excited ablated metal ions, M^{+*}, in determining reaction pathways [9,12]. Although the basis for the evident insignificance of M^{+*} from a source of nascent laser-ablated ions is not transparent, collisional cooling in the ablation plume might be an important factor. Early guided ion beam studies of reactions of selected Ln^+ with hydrocarbons by Sunderlin and Armentrout [13] suggested a minor role for excited-state ions even under conditions where significant concentrations of excited metal ions should have been present in the reaction zone.

The changing nature of the electronic structures of the actinides upon progressing across the series is of particular interest in illuminating both the distinctive behavior of elements of this series and the general relationships between the elements of the periodic table. Whereas the 4*f* electrons of the homologous lanthanide elements are essentially localized and chemically inert under most conditions, the electrons in the partially filled 5*f* orbitals of the lighter actinides, notably U, Np, and Pu, are sufficiently spatially extended and energetically proximate to those in the valence 6*d* and 7*s* orbitals that significant direct physical/chemical effects are evidenced [14]. A classic manifestation of the 5*f* electrons in bonding is in the distinctive and complex nature of Pu metal, which exists in at least five crystalline allotropic forms between 100°C and exhibits an anomalously low melting point of 640°C [15]. Beyond Pu in the actinide series, the behavior of these metals is largely reminiscent of that of the trivalent lanthanides, in accord with increasing stabilization/localization of the 5*f* electrons with increasing nuclear charge. However, manifestations of direct participation of 5*f* electrons in chemical bonding have been identified for transplutonium actinides, particularly under high pressure which decreases interatomic distances [16]. Furthermore, the increasing significance of relativistic effects on electronic structure, energetics and chemistry with increasing atomic number might result in novel properties for the heavier actinides [17].

Following early guided ion beam studies of U^+ gas-phase chemistry by Armentrout et al. [18], other FTICR-MS studies have been carried out on M^+ and MO^+ chemistries for M = Th and U [19–22]. Our initial actinide LAPRD studies were also performed with these two elements [23] and the results were in accord with those from FTICR-MS. Subsequently, the LAPRD approach was applied to sequentially investigate gas-phase chemistries of the first four transuranium actinide ions, $_{93}Np^+$, $_{94}Pu^+$ [24], $_{95}Am^+$ [25], and $_{96}Cm^+$ [26]. Rather than proceeding directly to the next element in the series, $_{97}Bk^+$, the present article reports on aspects of the gas-phase chemistry of $_{98}Cf^+$ (and CfO^+). The chemistry of Cf was assessed prior to that of the preceding element, Bk, to avoid potential ambiguities in interpretation of mass spectrometrical-based results for the latter, because ^{249}Bk decays to ^{249}Cf.

An emphasis of previous actinide LAPRD studies has been on organometallic ion chemistry, focusing on reactions of An^+ with alkenes. Based on studies with Ln^+ and lighter An^+, it has been found that a particularly reliable indicator of *f*-block element electronic structures, energy levels and resulting chemical activities is their comparative propensities to dehydrogenate alkenes:

$$M^+ + C_nH_m \rightarrow MC_nH^+_{m-2} + H_2 \quad (1)$$

These reactions evidently proceed via a rate-controlling step involving C–H bond activation by insertion (oxidative addition) of the metal ion into the hydrocarbon to produce a transient intermediate:

$$M^+ + R\text{–}H \rightarrow R\text{–}M^+\text{–}H \quad (2)$$

Subsequent abstraction of a neighboring H-atom resulting in H_2-elimination is presumably relatively facile, and the efficiency of these reactions for different M^+ is reflected in the mass-spectrometrically measured abundance of the resulting organometallic complex ions, depicted as $M^+ - \{C_nH_{m-2}\}$. For the Ln^+ and An^+ (with the possible exceptions of U^+ and some lighter actinide ions), the 4*f* and 5*f* electrons are evidently chemically inert and two non-*f* valence electrons at the metal center are required for reaction (2) to proceed [7,9-11]. Accordingly, the dehydrogenation activities of the studied *f*-block M^+ closely correlate with the energy necessary to achieve an electronic configuration comprising two unpaired non-*f* valence electrons, typically a $f^{n-2}d^1s^1$ valence electron configuration with a few exceptions such as Pr^+ where the $[Xe]4f^25d^2$ configuration, at 70 kJ-mol^{-1} above ground, lies ~24 kJ mol^{-1} below the $[Xe]4f^25d^16s^1$ configuration [27]. The relevant promotion energies to achieve a prepared "divalent" state (PE[M^+]) are plotted in Fig. 1 for the An^+, Np^+ through Cf^+, with values for Pr^+ and Tm^+ included for comparative purposes. The value in Fig. 1 for Cf^+ (250 kJ mol^{-1}) is only an estimate [29] whereas the other values were experimentally determined. The ground state of Cf^+ is $[Rn]5f^{10}7s^1$ and the lowest lying prepared divalent state is $[Rn]5f^96d^17s^1$. The estimated PE[Cf^+] is sufficiently large compared to those of reactive An^+, such as Cm^+ (PE[Cm^+] = 48 kJ mol^{-1}), that only minor dehydrogenation activity is predicted for Cf^+, if the estimated PE[Cf^+] is accurate and the conventional mechanistic model is applicable in this region of the actinide series.

In conjunction with the alkene reactions of central interest, other reagents were employed to explore new aspects of californium chemistry. Whereas alkanes are typically inert toward even the most reactive metal ions, at least under LAPRD conditions, hydrocarbon functionalization can strikingly enhance or diminish reactivity [30,31]; butyronitrile and butylamine were included here to assess this effect with Cf^+. Previous gas-phase metal ion reaction studies with thiols revealed unique chemistry normally not apparent in the condensed phase [32], and ethanedithiol was employed to synthesize gaseous californium sulfide and hydrosulfide complexes. Reactions with ethers were also investigated, to evaluate the Cf^+-induced C–O bond cleavage and prepare californium alkoxide complexes. Metal ion-induced abstraction of F atoms from perfluorocarbons has been shown to reveal the propensity for a given *f* element to exist in high oxidation states and offers a promising means for postionization chemical separation for mass spectrometric analysis of isobaric nuclides [33]; Cf^+ was reacted with hexafluoropropylene and perfluorophenanthrene.

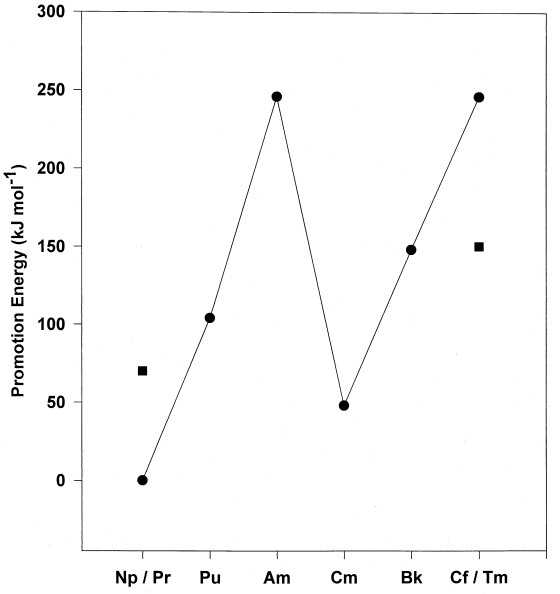

Fig. 1. Promotion energies for M^+ from the ground electronic state to the lowest-lying level of the lowest-energy "divalent" configuration with two non-*f* valence electrons: $5f^{n-2}6d^17s^1$ for the An^+, $4f^{12}5d^16s^1$ for Tm^+, and $4f^25d^2$ for Pr^+. The An^+ values (solid circles) are from Fred and Blaise [28], except for that for Cf^+ which is an estimate from Brewer [29]; the values for Pr^+ and Tm^+ (solid squares) are from Martin et al. [27].

2. Experimental

The LAPRD apparatus and experimental procedures used here have been described in detail elsewhere [7,23–26] and only a summary of key features of the approach are included here; details pertaining to

the californium experiments are provided. The attenuated 308 nm output of a XeCl excimer laser was focused to a ~0.5 mm^2 spot on a solid target containing the metals (as oxides) of interest. The nominal peak irradiance was ~10^8 W cm^{-2}, and ablated neutrals and ions propagated ~3 cm through a reactant gas injected either through a continuous leak valve (for liquid reagents) or a pulsed solenoid valve (for gaseous reagents). The pulsed valve was operated in synchronization with the laser at a repetition rate of 10 Hz, with the nominal valve-open interval typically set at 160 μs per pulse. Such intermittent gas introduction in harmonization with ion ablation is desirable because it provides much higher transient reagent pressures in the ion trajectory, and greater product yields. The quasisteady state reagent pressure measured downstream in the ion flight tube was comparable for the leak and pulsed valve experiments, and it is estimated that the pressure in the reaction zone was roughly 10^3 times greater for those reactant gases introduced through the pulsed valve. After a variable delay, typically t_d = 35 μs, positive ions present in the source region of the reflectron time-of-flight mass spectrometer were injected into the ion flight tube for mass analysis. For t_d = 35 μs, the approximate velocity of the sampled ions was 1 km s^{-1} (i.e. ~3 cm/35 μs); all ion–molecule reactions were carried out under hyperthermal conditions, and the center of mass collisional energies can be estimated from the ion velocity assuming quasistationary reactant molecules. The evidently minimal effects of the small hyperthermicity on comparative reactivities, and that the collisional energies were comparable for simultaneously studied reactant ions have been discussed previously [7,23–26,31]. The laboratory frame collisional energies for the Cf^+–molecule reactions were ~125 kJ mol^{-1}. However, the center-of-mass collisional energies (KE[CM]) were in the range of ~18 kJ mol^{-1} for propylene to ~90 kJ mol^{-1} for perfluorophenanthrene. The latter molecule is significantly more massive than the other studied reagents and all other KE[CM] were below 50 kJ mol^{-1}, most being substantially lower. Accordingly, most of the observed reactions are presumed to be nearly thermoneutral or exothermic.

The ^{249}Cf used in this work was obtained by means of β decay of ^{249}Bk produced in the High Flux Isotope Reactor at Oak Ridge National Laboratory. Californium-249 undergoes β decay with a half-life of 351 yr, and the rate of ingrowth of the ^{245}Cm daughter is 0.20% per year. The ^{249}Cf employed here had been chemically separated from its ^{245}Cm daughter five years prior to the LAPRD experiments, and ~1 at. % of the distinctive ^{245}Cm isotope (α-decay half-life = 8500 yr) was present in the target, resulting in detectable $^{245}Cm^+$ and $^{245}CmO^+$ peaks in the mass spectra; for some reactant gases, the reactivity of the co-ablated and relatively reactive Cm^+could be assessed. This afforded an opportunity for direct comparison of the chemistry of Cf^+ with that of Cm^+ and the ^{249}Cf target is referred to as "Cf(Cm)." An even less intense $^{243}Am^+$ peak was attributed to impurities introduced by the previous use of relatively large quantities of ^{243}Am in the apparatus. Am^+ has been shown to be quite unreactive toward the substrates studied here [25], and with the exception of small amounts of AmF^+ and AmF_2^+, no significant products from the reaction of Am^+ were identified in the present study.

As in earlier actinide studies [23–26], the targets were copper pellets (99.999% Cu) into which the metal oxides had been dispersed. The Cf(Cm) target was prepared using 1.5 mg of $^{249}Cf_2O_3$ (containing 15 μg of $^{245}Cm_2O_{\sim 3}$) and 16 mg of Cu, resulting in a composition of 2.1 at. % ^{249}Cf and 0.02 at. % ^{245}Cm, relative to Cu. Substantial variations in ion yields with translation of the target suggested compositional inhomogeneities on the scale of the laser beam.

A second ablation target, denoted as "PrTm" was mounted adjacent to the Cf(Cm) target on an *X–Y* translation stage. This configuration allowed comparing the chemistries of Pr^+ (and PrO^+) and Tm^+ with that of Cf^+ under virtually identical conditions. Although the co-ablated Tm^+ and Pr^+ (and PrO^+) were not ablated concurrently with Cf^+ and Cm^+, this experimental arrangement allowed for in situ target substitution, and sequential studies of the two targets were carried out with minimal changes in experimen-

tal conditions. The PrTm target was prepared using commercial oxide powders ($Ln_2O_{\sim 3}$, 99.9% purity). Both Pr and Tm exhibit a single naturally occurring isotope and the composition of the PrTm target was 2.1 at. % ^{141}Pr and 3.1 at. % ^{169}Tm, with the balance being Cu.

The liquid reagents were subjected to at least two freeze-evacuate-thaw cycles prior to use and the gaseous reagents were used directly from cylinders. The vendor-specified purities of the commercial reagents were as follows. Liquids: 98% 1,3-cyclohexadiene (C_6H_8); 99% cyclohexene (C_6H_{10}); 98% 1,3,5,7 cyclooctatetrene (C_8H_8, "COT"); 99.5% 1,5-cyclooctadiene (C_8H_{12}, "COD"); 99% butyronitrile (C_4H_7N); 99% butylamine ($C_4H_{11}N$); 90+% ethanedithiol ($C_2H_6S_2$); and mass spectrometer calibration grade perfluorophenanthrene ($C_{14}F_{24}$). Gases: 99.999% nitrous oxide (N_2O); 99% propene (C_3H_6); 99% 1-butene (C_4H_8); 95% trans-2-butene (C_4H_8); 99.8% dimethylether (C_2H_6O); 99% methylvinylether (C_3H_6O); and 99.5 % hexafluoropropene (C_3F_6).

3. Results and discussion

3.1. Oxides and hydroxides

Vacuum ablation of actinide oxides produces a qualitatively reproducible distribution of An^+, AnO^+ and, for some actinides, AnO_2^+ and/or $An(OH)^+$. It has been well-established [24] that the relative abundances of the directly ablated actinide molecular oxide ions reflects the stabilities of their oxides. The formal valence state, V_M, of a metal in an oxide, hydroxide or oxide-hydroxide ion, $M_xO_y(OH)_z^+$, is given by the relationship: $V_M = \{2y + z + 1\}/x$. Uranium normally exists in high oxidation states (>III), and accordingly UO^+ and UO_2^+ are the prevalent ablated species [34]. With the Cf(Cm) target, the ablated ions and representative approximate intensities (in millivolts) were as follows: Cf^+/1500; CfO^+/50; $Cf(OH)^+$/50; Cm^+/7; CmO^+/7; Am^+/6; and AmO^+/5. As expected, CfO^+ is clearly less stable than both CmO^+ and AmO^+. Similarly, a typical abundance distribution from the PrTm target was: Pr^+/50; PrO^+/450; Tm^+/300; TmO^+/0.7; and $Tm(OH)^+$/0.7. In addition, the following small californium oxide cluster ions were ablated from the Cf(Cm) target: Cf_2O^+/0.9; $Cf_2O_2^+$/2.7; $Cf_2O_2(OH)^+$/0.4; $Cf_3O_3^+$/0.06; $Cf_3O_4^+$/0.23. In contrast to the lighter actinides, U, Np,and Pu, no species comprising Cf in an oxidation state greater than +3 were identified.

In an attempt to oxidize An^+ to AnO^+, nitrous oxide was admitted into the reaction zone through the pulsed gas valve. The amounts of directly ablated AmO^+ and CmO^+ precluded detection of any post-ablation oxidation of Am^+ and Cm^+. In contrast, directly blated CfO^+ was a minor constituent, but no evidence was obtained for the oxidation reaction, $Cf^+ + N_2O \rightarrow CfO^+ + N_2$. Thermodynamic considerations suggest that Am^+, Cm^+, and Cf^+ should abstract an O atom from N_2O to produce the AnO^+. Specifically, the enthalpy associated with the reaction, $N_2O \rightarrow N_2 + O$, is only 165 kJ mol^{-1} [35] whereas the association reactions, $An + O \rightarrow AnO$, have enthalpies ranging from -500 kJ mol^{-1} for Cf (estimated) to -730 kJ mol^{-1} for Cm [36]. The dissociation energies, $D°$, of the neutral and monopositive lanthanide monoxides, LnO and LnO^+, are comparable to one another for a given Ln [37], and a similar correspondence is anticipated between the AnO and AnO^+ dissociation energies. Accordingly, it is expected that the gas-phase oxidation reactions for the actinide ions, $An^+ + N_2O \rightarrow AnO^+ + N_2$, should be appreciably exothermic. The kinetic inefficiency of N_2O at oxidation of Cf^+ is consistent with results obtained previously by other researchers, including Armentrout et al., and Ritter and Weisshaar [38]. The barrier to oxidation is considered to be related to the necessity for spin conservation between N_2O and $\{N_2 + O\}$. Strong M^+–O bonding can lower the activation barrier for N_2O decomposition. Such an effect was indicated by a FTICR-MS study of the oxidation of Ce^+ and Nd^+ to LnO^+ by N_2O [39] which demonstrated the formation of CeO^+ ($D° = 850$ kJ mol^{-1} [37]) with approximately twice the efficiency of that of NdO^+ ($D° = 750$ kJ mol^{-1}).

3.2. Reactions with alkenes

The primary results for reactions of ablated ions with alkenes are summarized in Table 1, and with other reagents in Table 2. Representative product mass spectra for reactions of Cf^+, Cm^+, Pr^+, and Tm^+ with 1-butene are shown in Fig. 2. In both of the results Tables 1 and 2, the product yields are expressed as abundances relative to the remaining reactant ion; most yields were minor (e.g. <20%) relative to the amount of unreacted ion. Where only an upper limit is given for a product's abundance, the complex ion was not detected in the mass spectrum. Due to the minor amount of Cm^+ ablated, typically ≪5% relative to Cf^+, only limited results are presented for curium.

In addition to the alkenes specified in Table 1, the four studied metal ions were reacted with COD. In accord with results for other alkenes, a significantly reduced reactivity of Cf^+ was indicated as compared with Pr^+ and Tm^+, specifically, no Cf^+–L products were detected whereas both Pr^+–C_8H_8 and Tm^+–C_8H_8 were produced. Reaction products from the minor amount of ablated Cm^+ were not discernable with COD. In accord with previous results for LnO^+ and AnO^+, no reaction products resulted from reactions of oxo-ligated metal monopositive ions with alkenes. It is not energetically feasible to achieve an electronic configuration at the metal center in these MO^+ comprising two non-*f* valence electrons and evidently noninsertion, multicentered hydrocarbon dehydrogenation processes proceed only very inefficiently.

For each of the three small (normally gaseous) alkenes, Cm^+ and Pr^+ induced dehydrogenation whereas Cf^+ and Tm^+ were inert within the detection limits. It was found that Cm^+ was at least 400 times more reactive than Cf^+, and Pr^+ at least 40 times more reactive than Tm^+. A qualitative comparison of the results for Cm^+ and Pr^+ suggests a somewhat greater reactivity for the actinide ion. These results are in accord with the C–H activation/H_2-elimination model outlined previously and the energies indicated in Fig. 1, which are required to achieve divalent configurations of the *f*-element ions prior to insertion into a C–H bond; the ordering is: Cf^+/250 kJ mol^{-1} (estimated) > Tm^+/199 kJ mol^{-1} > Pr^+/70 kJ mol^{-1} > Cm^+/48 kJ mol^{-1}. The

Table 1
Product distributions for alkene reagents[a]

Propylene[b]	$I[M^+]$	$A[MC_3H_4^+]$ $(+H_2)$
Cf^+	920	<0.01
Cm^+	5.9	4.1
Pr^+	720	0.8
Tm^+	440	<0.02
1-Butene[b]	$I[M^+]$	$A[MC_4H_6^+]$ $(+H_2)$
Cf^+	1630	<0.003
Cm^+	4.7	19
Pr^+	310	2.0
Tm^+	290	<0.05
Trans-2-butene[b]	$I[M^+]$	$A[MC_4H_6^+]$ $(+H_2)$
Cf^+	1890	<0.005
Cm^+	6	18
Pr^+	500	1.1
Tm^+	530	<0.02
1,3-Cyclohexadiene[c]	$I[M^+]$	$A[MC_6H_6^+]$ $(+H_2)$
Cf^+	1200	0.01[d]
Pr^+	360	0.13
Tm^+	490	0.08
Cyclohexene[c]	$I[M^+]$	$A[MC_6H_6^+]$ $(+2H_2)$
Cf^+	850	<0.01
Pr^+	380	0.4
Tm^+	480	<0.01
1,3,5,7-Cyclooctatetraene[c,e]	$I[M^+]$	$A[MC_8H_8^+]$ (adduct)
Cf^+	1200	0.2
Pr^+	140	0.1
Tm^+	430	0.6

[a] Peak heights, *I*, are for unreacted ions, in mV; results are similar using peak areas. The product abundance, *A*, is the amount of product ion, M^+–L*, relative to the total amount of unreacted and product ions, M^+–L: $A[M^+–L^*] = \{I[M^+–L^*]/(I[M^+] + \Sigma\{I[M^+–L]\})\} \times 100$. No adducts/products were identified for any MO^+. Cm^+ results are included where $I[Cm^+]$ was sufficient to produce detectable products. Some minor or indeterminate products are excluded.

[b] Pulsed-value reagent (cylinder gas).

[c] Leak-value reagent (liquid).

[d] Product ion intensity close to detection limit.

[e] t_d = 40 μs; t_d = 35 μs for all other alkenes.

Table 2
Product distributions for nonalkene reagents[a]

Butyronitrile	$I[M^+]$	$A[M^+–C_4H_7N]$[b] (adduct)
Cf^+	600	0.5
Pr^+	130	1.1
Tm^+	290	6.2
CfO^+	4	23
PrO^+	350	11
TmO^+	1.0	<20

Butylamine	$I[M^+]$	$A[M^+–C_4H_{11}N]$	$A[M^+–C_4H_{8,9}N]$[c]	$A[M^+–C_4H_7N]$
Cf^+	2600	0.36	0.17	<0.05
Pr^+	96	0.2	<0.1	0.9
Tm^+	390	0.7	0.13	<0.03
PrO^+[d]	750	0.8	0.07	0.05

Ethanedithiol	$I[M^+]$	$A[MS^+]$	$A[MSH^+]$	$A[MS_2^+]$	$A[M(SH)_2^+]$
Cf^+	1200	0.5	0.4	0.11	0.23
Pr^+	73	4.7	0.8	1.8	<0.3
Tm^+	330	1.1	0.5	1.7	0.8

Dimethylether	$I[M^+]$	$A[M^+–CH_3OCH_3]$	$A[M^+–OCH_3]$	$A[M^+–(OCH_3)_2]$
Cf^+	890	0.02	0.06	<0.05
Cm^+	5.2	<0.05	45	3.3
Pr^+	190	<0.05	1.9	0.4
Tm^+	410	0.05	0.5	<0.05

Hexafluoropropene[e]	$I[M^+]$	$A[MF^+]$	$A[MF_2^+]$
Cf^+	310	2.2	0.13
Cm^+	6.2	13	4.5
Am^+	6.5	11	2.6
Pr^+	290	2.7	1.1
Tm^+	210	1.6	0.4

Perfluorophenanthrene[e]	$I[M^+]$	$A[MF^+]$	$A[MF_2^+]$
Cf^+	210	15	0.24
Cm^+	10	29	3
Pr^+	160	60	1.9
Tm^+	310	0.9	0.08

[a] Peak heights, *I*, are for unreacted ions, in millivolts. The product abundance, *A*, is the amount of product ion, M^+–L* (or MO^+–L), relative to the total amount of unreacted and product ions, M^+–L (MO^+–L): $A[M^+–L^*] = \{I[M^+–L^*]/(I[M^+] + \Sigma\{I[M^+–L]\})\} \times 100$. Results for Cm^+ are included only where $I[Cm^+]$ (or $I[CmO^+]$) was sufficient to produce detectable products. Some minor or indeterminate products are not included. Where products of reactions with MO^+ are included, the ''M^+'' in ''$I[M^+]$'' and ''$A[M^+]$'' should be taken to designate MO^+.

[b] For Pr^+, an $A[C_4H_5N] = 0.7$ peak was additionally evident.

[c] $M^+–C_4H_9N$ for M = PrO; $M^+–C_4H_8N$ for M = Cf and Tm; neither product detected for M = Pr.

[d] No products detected for CfO^+ (I = 17 mV) or TmO^+ (I = 0.5 mV).

[e] No MOF^+ or MOF_2^+ were detected.

low reactivity of Cf^+ indicates that excited state Cf^{+*} ions were minor participants and, more significantly, that the quasivalence 5*f* electrons of Cf^+ are chemically inert and do not participate directly in C–H activation.

The results for the four liquid alkenes, the three included in Table 1 and COD, also indicated a particularly low reactivity for Cf^+. Presumably due to the relatively low reagent pressures achieved under constant flow conditions, no Cm^+ reaction products

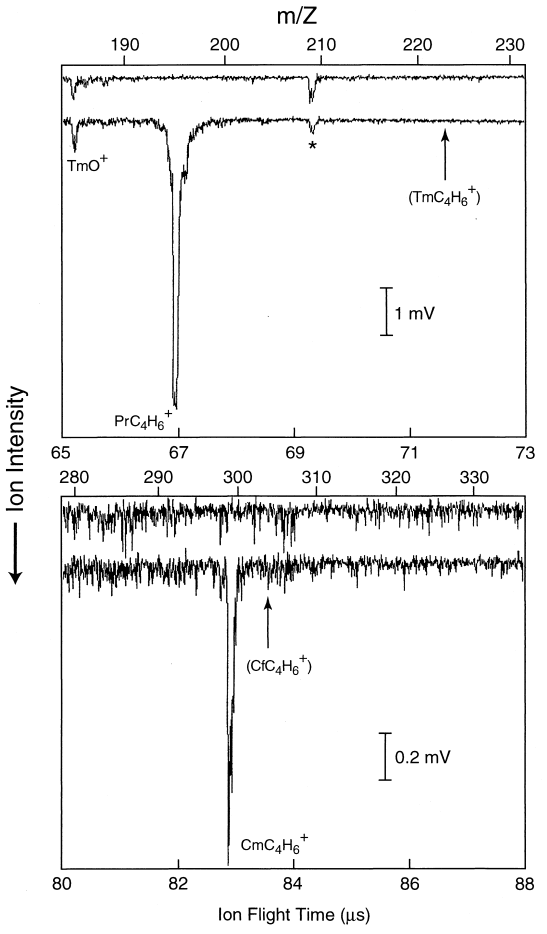

Fig. 2. Mass spectra for ablation of the Pr/Tm (top) and Cf(Cm) (bottom) targets into 1-butene, C_4H_8; the two spectra shown for each target are for the pulsed valve closed (top scan) and open (bottom scan). The intensities (in millivolts) of some peaks not shown are: Pr^+/310; PrO^+/800; Tm^+/290; Cm^+/4.7; CmO^+/3.5; Cf^+/1630; CfO^+/3.2. The asterisked peak at 209 Da was evident in most Pr/Tm ablation spectra, with or without a reactant gas, and may be due to a Bi impurity in this target. Species cited in parentheses were not detected.

were evident. A very minor degree of cyclohexadiene dehydrogenation to produce $CfC_6H_6^+$ (probably a Cf^+–benzene complex in view of the low cracking activity of Cf^+) may have occurred, although the abundance was barely above the detection limit. Otherwise, Cf^+ was inert toward dehydrogenation and only the Cf^+–COT adduct was detected. In view of this inert character of Cf^+, it is reasonable to conclude that the $CfC_8H_8^+$ product from the $Cf^+ + C_8H_8$ reaction is indeed an adduct rather than a product requiring C–C activation, such as {benzene–Cf^+–acetylene}. The results with cyclohexadiene and cyclohexene (as well as COD) again indicated a greater dehydrogenation activity for Pr^+ as compared with Tm^+. The results with cyclohexadiene suggest, somewhat more qualitatively, a greater C–H activation efficiency for Tm^+ as compared with Cf^+, consistent with a PE[Cf^+] greater than 200 kJ mol^{-1}, in accord with the estimated value of ~250 kJ mol^{-1} from Brewer [29]. The M^+–COT adduct abundances for Cf^+, Pr^+, and Tm^+ were sufficiently similar that definitive quantitative comparisons could not be asserted.

The only crystallographically characterized organocalifornium compound is the π-bonded ionic compound, californium-tris-cyclopentadienyl [$Cf(C_5H_5)_3$], which comprises nominally trivalent Cf and reflects the lanthanidelike character of Cf [40–43]. In the present work, two π-bonded organocalifornium complexes have been identified: $[Cf–COT]^+$ (formally Cf^{3+}–COT^{2-}) and, with less certainty, $[Cf–benzene]^+$ (formally Cf^+–$benzene^0$). The apparent stability of the Cf–COT "half-sandwich" complex is noteworthy in view of the seminal preparation of the π-bonded sandwich compound uranocene, formally COT^{-2}–U^{4+}–COT^{2-}, by Streitweiser and Muller-Westerhoff [44]. The latter accomplishment accelerated the development of organometallic chemistry of actinides, especially that of thorium and uranium. The preparation described here of what is presumed to be the half-sandwich complex, Cf^{3+}–COT^{2-}, suggests that it may be feasible to prepare solid, ionic californium compounds such as $CfClC_8H_8$ (Cl^-–Cf^{3+}–COT^{2-}). However, it is noted that no such analogous lanthanide compounds have been reported.

3.3. Reactions with butyronitrile and butylamine

The primary results for reactions with butyronitrile, CH_3–CH_2–CH_2-C≡N, and butylamine, CH_3–CH_2–CH_2–CH_2–NH_2, are included in Table 2, and representative product mass spectra for ablation of both the Cf(Cm) and PrTm targets into butylamine are shown in Fig. 3. When butyronitrile was used, the

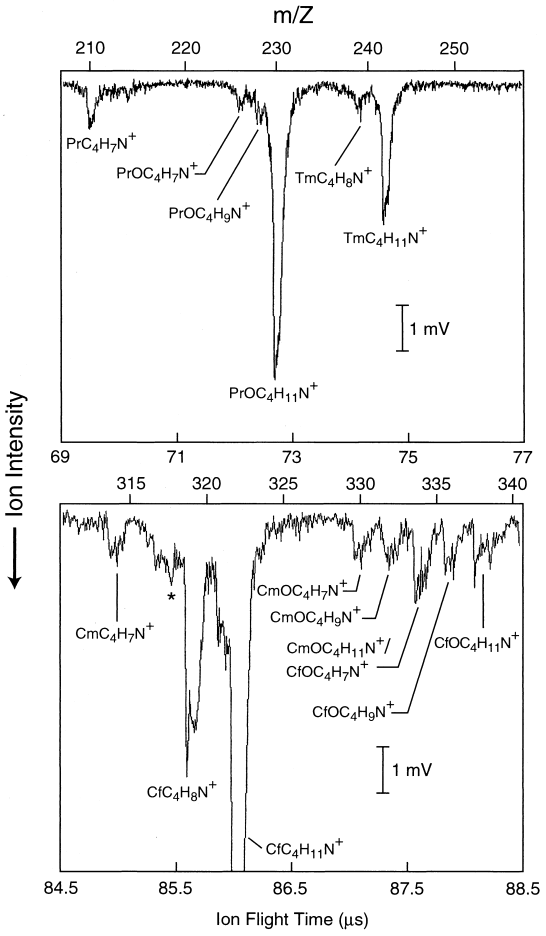

Fig. 3. Mass spectra for ablation of the Pr/Tm (top) and Cf(Cm) (bottom) targets into butylamine, $C_4H_{11}N$. The simultaneously measured unreacted parent ion intensities (millivolts) were as follows: Pr^+/96; PrO^+/750; Tm^+/390; TmO^+/0.5; Cm^+/6.9; CmO^+/7.4; Cf^+/2600; CfO^+/18. No products derived from TmO^+ were detected. The small asterisked peak in the bottom spectrum can be assigned to $CmC_4H_{10}N^+$, $CfC_4H_6N^+$, or some indeterminate species. The intensity of the $CfC_4H_{11}N^+$ peak, off-scale in this spectrum, was approximately twice that of the neighboring $CfC_4H_8N^+$ peak.

primary complex ions were what are presumed to be adducts, having the compositions $MC_4H_7N^+$. As indicated in footnote b of Table 2, only with Pr^+ was a dehydrogenation product, $PrC_4H_5N^+$, detected; this accords with the relatively small PE[Pr^+] and the ability of Pr^+ to insert into a C–H bond, following its coordination to the terminal C≡N: functionality. The mode of metal ion coordination to the nitrile functionality which precedes insertion may involve the C≡N π-bonding system, rather than the terminal N: lone pair of electrons; such a M^+–η^2-C≡N configuration would place the metal ion in proximity to the target CH_2 group adjacent to the nitrile group and enable insertion into a neighboring C–H bond. In analogy with our COT results, it appears that Tm^+ is somewhat more effective at coordinating butyronitrile than is Cf^+. This difference may reflect that the effective ionic radius of Tm^+ is probably smaller than that of Cf^+, as a result of two effects: actinide cations exhibit greater radii than the homologous lanthanide cations; and lanthanide/actinide radii contraction occurs upon progressing across each series [45]. The terminal N: functionality is a relatively hard electron donor and may coordinate more effectively with the Tm^+, given its smaller charge-to-size ratio. As discussed previously [31], the greater propensity for MO^+, compared to naked M^+, to coordinate to a nitrile probably reflects the greater effective positive charge at the metal center in MO^+. As with alkenes, the absence of dehydrogenation activity for the MO^+, despite appreciable adduct formation, is attributed to the dearth of non-*f* valence electrons, or easily promotable *f* electrons, at the metal center in the MO^+ for participation in C–H activation via an oxidative insertion process.

Greater reactivity of ablated ions was evidenced with butylamine compared with butyronitrile, in accord with previous results for other actinides [31]. The three bare metal ions, Cf^+, Pr^+, and Tm^+, as well as the abundant oxide ion, PrO^+, each formed adducts with butylamine. Double-dehydrogenation to produce C_4H_7N, presumably butyronitrile, was induced by Pr^+ and PrO^+. The single-H_2-loss product also appeared with PrO^+: $PrOC_4H_9N^+$. The dehydrogenation mechanism for the oxide ion likely involves a multicentered intermediate [31]. It is assumed that insufficient CfO^+ and TmO^+ were ablated to result in detectable dehydrogenation. A contrasting mechanism involving insertion of Pr^+, electrostatically coordinated to the N: lone electron pair, into a C–H or N–H bond is consistent with the greater dehydrogenation activity of Pr^+ compared to Cf^+ (and Tm^+). An unanticipated result was the appearance of the 3H-loss channel distinctly for Cf^+ and Tm^+; this

pathway was not apparent in previous LAPRD studies with butylamine, including for its reaction with Tm^+ [31]. The mass resolution of the Cf^+ + butylamine spectrum was rather poor [Fig. 3(bottom)]. However, the dominant peak is confidently assigned as the adduct, $CfC_4H_{11}N^+$. The mass separation between this and the preceding large peak is confidently assigned as $\Delta m/z = 3$ (not 2 or 4) and accordingly the assignment of $CfC_4H_8N^+$, rather than the presumably more plausible $CfC_4H_9N^+$ ($\Delta m/z = 2$) or $CfC_4H_7N^+$ ($\Delta m/z = 4$), is virtually certain. Evidently, insertion into a N–H (or C–H) bond of the Pr^+ metal center coordinated to the single-H_2-loss complex, $PrC_4H_9N^+$ (Pr^+–{:NH=CH–C_3H_7}) was sufficiently facile that double dehydrogenation was the dominant pathway. Whereas Pr^+ can evidently achieve the requisite prepared divalent configuration, 70 kJ mol^{-1} above ground, to enable the second insertion, coordination of higher promotion energy ions, such as $Cf^+$and Tm^+ (PE≳200 kJ mol^{-1}), to the C=N: funtionality of butylimine, CH_3–CH_2–CH_2–CH=NH, may result in atomic H loss from the nitrogen and formation of σ-bonded complexes: M^+–N=CH–C_3H_7. The ground state configurations of Cf^+ ([Rn]$5f^{10}7s^1$) and Tm^+ ([Xe]$4f^{13}6s^1$) both include a lone electron in the valence *s* orbital, which should effectively participate in formation of a single M^+–N σ-type bond. These species may be stabilized by allylic character in the M^+–N=C portion of the complex. The somewhat hyperthermal nature of the observed processes precludes assessment of the M^+–N bond strength in the postulated complexes but the requisite N–H bond cleavage should require at least ~400 kJ mol^{-1} (e.g. NH_3 + 455 kJ mol^{-1} → NH_2 + H [35]). In comparison, $D°[Sc^+–NH_2] \approx 350$ kJ mol^{-1} [1]; Sc is a quasilanthanide element and roughly similar dissociation energies might be anticipated for Ln^+–N and An^+–N single bonds.

3.4. Reactions with ethanedithiol and ethers

The results for reactions of ablated ions with ethanedithiol are included in Table 2, and product ion mass spectra for ablation of the Cf(Cm) and PrTm targets into this reagent are shown in Fig. 4. The

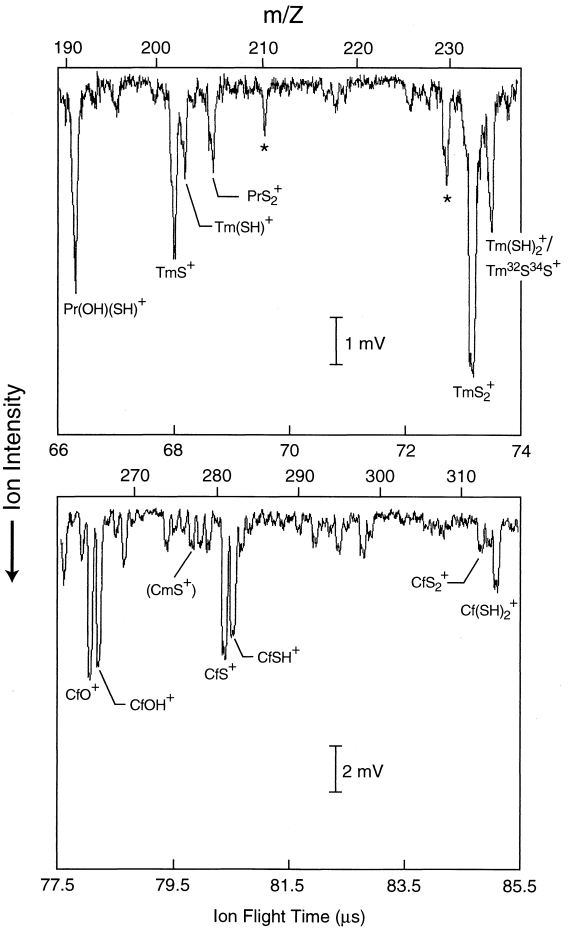

Fig. 4. Mass spectra for ablation of the Pr/Tm (top) and Cf(Cm) (bottom) targets into ethanedithiol, $C_2H_6S_2$. The intensities (millivolts) of some peaks not shown are: Pr^+/73; PrO^+/~600; Tm^+/330; TmO^+/1.5; $TmOH^+$/1.8; PrS^+/3.7; $PrSH^+$/0.5; $Pr(SH_2)^+$/2.4; Cm^+/4; CmO^+/6; Cf^+/1200. The asterisked peaks in the top spectrum correspond to $PrC_4H_7N^+$ at 210 Da and $PrOC_4H_{11}N^+$ at 230 Da, probably resulting from reaction with residual butylamine which was the reagent admitted immediately prior to the ethanedithiol studies.

primary products appear to have resulted from abstraction of one or two S atoms or SH ligands by the naked metal ions. As discussed in greater detail elsewhere [32], concerted loss of S_2 from a single $C_2H_6S_2$ molecule, leaving an ethane residual, requires only 50 kJ mol^{-1}, and the loss of two SH moieties, leaving an ethene residual, requires 340 kJ mol^{-1}. Although thermodynamically favorable, concerted loss of S_2 from ethanedithiol may be kinetically

unreasonable. An alternative pathway is formation of $\{C_2H_4 + H_2 + S_2\}$, a process requiring 186 kJ mol^{-1} [32,35]. The product distribution is thermodynamically plausible (even neglecting the hyperthermicity of the reaction conditions) for these unimolecular processes, if 50 kJ mol^{-1} or 186 kJ mol^{-1} (depending on the mechanism) can be recouped by formation of a M^+–S_2 persulfide bond (M^+–η^2–{S–S}), and 340 kJ mol^{-1} in the formation of the two hydrosulfide bonds in HS–M^+–SH. Abstraction of a single S atom, leaving an ethanethiol residual, requires 240 kJ-mol^{-1}, and M^+=S bonds are sufficiently strong to enable this process. Finally, abstraction of a single SH moiety from ethandedithiol probably requires at least ~300 kJ mol^{-1} [32]. Although very little thermodynamic information is available on metal hydrosulfide molecular thermodynamics, Barsch et al. recently investigated the iron hydrosulfide system and determined $D°[Fe^+–SH] = 276(11)$ kJ mol^{-1} [46]. Although hydroxide bonding is likely somewhat stronger than hydrosulfide bonding, $D°[Sc^+\text{-}(OH)] \approx 500$ kJ mol^{-1} [1] and it is certainly feasible that $D°[Cf^+–(SH)]$ is greater than 300 kJ mol^{-1}. Although the bonding between an electropositive metal and sulfur should generally be weaker than that between the metal and oxygen, the decrease is not expected to be so great as to preclude (SH) abstraction. For example $D°[Mg=S] = 278$ kJ mol^{-1} is only ~20% less than $D°[Mg=O]$ [47]. Whereas the abundances of the divalent species, MSH^+, were comparable for M = Cf, Pr, and Tm, the yields of the trivalent species, MS^+ and $MS_2{}^+$ (the latter is presumed to incorporate a metallacyclic persulfido structure and a nominally trivalent metal center [32]) were smaller for Cf than for Pr and Tm. This is consistent with the greater propensity for Cf to exist in the divalent state [41], even to a greater degree than Tm, and is also consistent with the M^+ promotion energies cited above and in Fig. 1. Because the ionization energies of Cf^{2+} [48] and Tm^{2+} [27] are virtually identical (~2280 kJ mol^{-1}) the evidently greater stabilities of the trivalent Tm sulfide, TmS^+ and particularly $TmS_2{}^+$, and hydrosulfide, $Tm(SH)_2{}^+$, complexes compared to the corresponding trivalent Cf complexes suggests appreciable covalent metal–sulfur bonding, in contrast to more highly ionic metal-oxygen bonding. The absence of detectable $Pr(SH)_2{}^+$ might be attributable to a relatively high stability of the monosulfide, Pr^+=S, in direct analogy to the stability of the corresponding monoxide. Relevant dissociation energies (in kJ mol^{-1}) are as follows [37]: $D°[Pr–S] = 470$; $D°[Pr–O] = 790$; $D°[Pr^+–O] = 750$; $D°[Tm–O] = 510$; $D°[Tm^+–O] = 480$; and $D°[Cf–O] \approx 500$, the last as estimated by Haire [36]. The CfS^+, $CfS_2{}^+$, $CfSH^+$, and $Cf(SH)_2{}^+$ complexes synthesized here represent the first such gaseous sulfide and hydrosulfide molecular species of Cf. The hydrosulfide species are particularly unusual and are of special interest for analogy with prevalent hydroxide vapor species; in this regard, $CfOH^+$ was a prominent directly ablated ion.

The results for reactions of ablated ions with dimethylether are included in Table 2 and product mass spectra for the Cf(Cm) and PrTm targets are shown in Fig. 5. The results for methylvinylether, CH_3–O–CH=CH_2, are not tabulated but were in accord with those for dimethylether. In particular, only the divalent californium mono-alkoxide, $Cf(OCH_3)^+$, was identified whereas the trivalent curium hydroxide alkoxide, $Cm(OH)(OCH_3)^+$, was a significant product. Some other, complex and indeterminate products were detected with methylvinylether [32] but these did not provide conclusive additional insights into distinctive chemical behavior of Cf^+. Whereas both Cf^+ and Tm^+ produced measurable amounts of the condensation product with dimethylether, M^+–{CH_3OCH_3} (which is presumed to be a simple adduct), Cm^+ and Pr^+ were evidently so reactive that detectable amounts of the intact ether molecule coordinated to these metal ions were not retained. In addition to the condensation products, Cf^+ and Tm^+ reacted to give small amounts of the methoxide, M^+–OCH_3, in which the metal center is formally divalent. In comparison, Cm^+ and Pr^+ were substantially more reactive, with the abundance of the mono-methoxide complex ion being almost 10^3 times greater for Cm^+ than Cf^+. Because both Cm^+ and Cf^+ possess the requisite single non-*f* valence electron in their ground state to form a M^+–O covalent bond and have essentially identical ionization energies (1200 kJ mol^{-1} [48]), the bonding

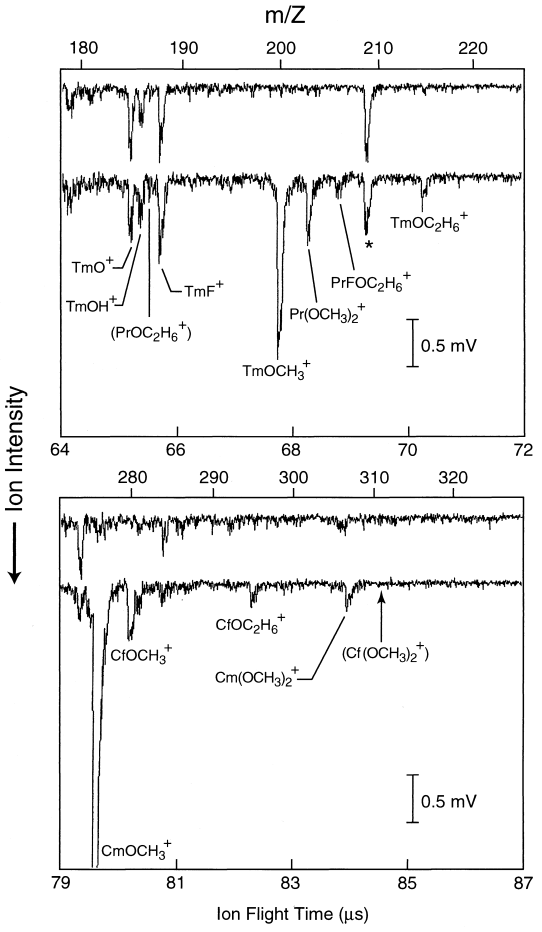

Fig. 5. Mass spectra for ablation of the Pr/Tm(top) and Cf(Cm) (bottom) targets into dimethyl ether, C_2H_6O; the two spectra for each target are for the pulsed valve off (top scan) and on (bottom scan). The intensities (millivolts) of some peaks not shown are: Pr^+/190; PrO^+/840; $PrOCH_3^+$/4.7; Tm^+/410; $Tm(OCH_3)_2^+$/ $<$0.05 (not detected); Cm^+/5.2; CmO^+/5.1; Cf^+/890; CfO^+/3.6. The asterisked peak was pervasive and corresponds to 209 Da, perhaps a $^{209}Bi^+$ impurity.

thermodynamics in An^+–OCH_3 should be similar for both An^+ regardless of the degree of ionicity. Accordingly, differences in their behaviors are attributed to mechanistic effects. As with C–H (and C–C) activation, it can be inferred that dimethylether cleavage proceeds most effectively by insertion of a metal center, M^+, into a C–O bond to produce a H_3C–M^+–OCH_3 intermediate, which then eliminates a methyl radical to produce the methoxide product ion. The stability of the latter product is attributed to the high oxophilicity of the electropositive actinide (and lanthanide) metals. That neither Cf^+ nor Tm^+ produced detectable amounts of the bis-methoxide products, $M^+(OCH_3)_2$, can be attributed to the dearth of the mono-methoxide precursor, and the resistance of theses two particular *f* elements toward oxidation to the trivalent state. Both the promotion energies (leading to covalent bonding) and third ionization energies (ionic bonding) are relatively unfavorable for formation of these trivalent bis-methoxides. In contrast, both Cm^+ and Pr^+ produced significant amounts of M^+–$(OCH_3)_2$. Although both of these metal ions have sufficiently small promotion energies that their trivalent species should be more accessible, the above-postulated insertion mechanism is precluded for the M^+–(OCH_3) precursor complex where only a single valence electron is accessible at the metal center as a result of relatively low-energy electronic excitation. Insertion of the M^+–(OCH_3) precursor into a C–O bond to form the bis-methoxide product accordingly is not feasible. It may be that abstraction of an OCH_3 moiety from a second dimethylether molecule occurs via an alternative mechanism, but another possible scenario involves a concerted, multicentered fragmentation or coordination of a single H_3C–O–CH_3 molecule by MO^+. Ablated CmO^+ and PrO^+ were both abundant and the "M^+–$(OCH_3)_2$" may actually correspond to MO^+–(CH_3OCH_3) adducts. Regarding the chemistry of Cf, the central conclusion is that formation of even the mono-alkoxide is inefficient, and the trivalent bis-methoxide was not detectable. Among the few californium compounds whose volatility have been investigated is the homoleptic chelate-type complex in which three organic moieties are coordinated to Cf through C–O^- functionalities [41,49], californium tris-dipivaloylmethanato [$Cf(dpm)_3$], the formal fully ionic representation of the two resonance structures of which are: $Cf^{3+}[(CH_3)_3CCO^-CHCOC(CH_3)_3]_3 \leftrightharpoons Cf^{3+}[(CH_3)_3CCOCHCO^-C(CH_3)_3]_3$. The composition of this complex was only inferred from tracer-level studies and it was concluded that the volatility of $Cf(dpm)_3$ is less than that of the preceding $An(dpm)_3$ [49]. Based upon the LAPRD results, it appears that, in comparison with preceding actinides, it will prove be more difficult

Table 3
Ionization energies (kJ mol^{-1}) [27, 48]

	IE[M^+]	IE[M^{2+}]	IE[M^{3+}]
Am	1160	2130	3490
Cm	1200	2020	3550
Cf	1200	2270	3600
Pr	1020	2080	3760
Tm	1160	2280	4120

to synthesize volatile (trivalent) californium alkoxides; furthermore, the vapor pressures of such species might be at least somewhat lower than those of lighter actinide tris-alkoxides, in accord with the dpm results.

3.5. Reactions with fluorocarbons

Reactions of electropositive metals with fluorinated hydrocarbons to produce metal fluorides is considered to proceed via a "harpoon" mechanism, whereby charge transfer to the highly electronegative fluorine atom ($C–F^{\delta-}\cdots M^{(1+\delta)+}$) precedes its abstraction by the metal ion, and no insertion (direct C–F bond activation) is involved [50]. According to this mechanistic scenario, the propensity for a metal ion, M^+, to abstract a F atom from a fluorocarbon should correlate with its ionization energy, IE[M^+]; the propensity for a MF^+ ($\sim M^{2+}F^-$) to abstract a second F atom to produce MF_2^+ should correlate with IE[M^{2+}]; etc. Relevant ionization energies are given in Table 3.

With hexafluoropropene (C_3F_6) and perfluorophenanthrene ($C_{14}F_{24}$, with which AmF_n^+ ions were not detected, presumably due to the low vapor pressure of the reactant), the orderings of fluoride product abundances (Table 2) for the two targets were as follows ("$\gtrsim$" indicates abundances within a factor of 2; "$>$" indicates abundances within a factor of 10; and "$\gg$" indicates abundances differing by greater than a factor of 10). Cf(Cm) C_3F_6 and $C_{14}F_{24}$: CmF^+ ($\gtrsim AmF^+$) $> CfF^+$ CmF_2^+ ($\gtrsim AmF_2^+$) $\gg CfF_2^+$ (AmF_n^+ only for C_3F_6). PrTm C_3F_6: $PrF^+ \gtrsim TmF^+$ $PrF_2^+ > TmF_2^+$. $C_{14}F_{24}$: $PrF^+ \gg TmF^+$ $PrF_2^+ \gg TmF_2^+$. In contrast to actinides such as uranium, no tetravalent products such as MOF^+ or MF_3^+ were detected, reflecting the relatively large fourth ionization energies of the studied *f* elements. Compare the IE[M^{3+}] in Table 3 with IE[U^{3+}] = 3140 kJ mol^{-1} [48] in the context that both UF_3^+ and UOF^+ were produced upon ablation of a uranium target into hexafluoropropene [26]. For the actinide ions, the monofluoride abundances did not differ greatly. As seen in Table 3, the IE[An^+] for Am, Cm, and Cf are similar and accordingly only a relatively small difference in the AnF^+ abundances were discerned. In contrast, the abundance of CfF_2^+ was substantially below that of CmF_2^+ (and below that of AmF_2^+ upon reaction with C_3F_6). This latter result is in accord with the significantly larger value of IE[Cf^{2+}] compared with IE[Cm^{2+}] (and IE[Am^{2+}]) and is consistent with the known stability of the divalent state of Cf [41]. The results for the PrTm target were notable in that the abundance distributions were rather discrepant between the C_3F_6 and $C_{14}F_{24}$ reagents. Presuming that formation of MF_2^+ proceeds primarily by discrete abstraction of a second F atom by a MF^+ precursor (concerted abstraction of two F atoms from a single molecule would result primarily in MF_2^+ products), the relatively low yield of TmF_2^+ from $C_{14}F_{24}$ is attributed to both the dearth of TmF^+ precursor and the larger IE[Tm^{2+}]. The basis for the evidently very large discrepancy between C_3F_6 and $C_{14}F_{24}$ in single-F-atom abstraction by Pr^+ and Tm^+ warrants further consideration. Cornehl, et al. [50] found a very low F-abstraction efficiency ($\lesssim$1%) for Tm^+ compared with Pr^+ with a variety of fluorocarbons. Thus, although the formation of the monofluoride ions, MF^+, may be thermodynamically favorable for both Tm^+ and Pr^+, the reaction rate is substantially lower for Tm^+, presumably reflecting a lesser facility of charge transfer from Tm^+, with its larger ionization energy, and resulting lower efficiency of the harpoon-abstraction process. In the LAPRD experiments, the pressure of C_3F_6 was much greater than that of $C_{14}F_{24}$ and such mechanistic limitations to achieving the thermochemically stable products were evidently manifested to a much greater degree under conditions where fewer ion-molecule collisions occurred, i.e. with $C_{14}F_{24}$. Because IE[Cf^+] and IE[Cm^+] are nearly identical, the degree of formation of CfF^+ and CmF^+ are evidently more similar regard-

less of the average number of ion–molecule collisions; only in the inefficient formation of CfF_2^+ does the difference appear because IE[Cf^{2+}] is substantially greater than IE[Cm^{2+}]. These results provide an illustration how kinetic effects can be employed to control the extent of gas-phase reactions and potentially achieve postionization chemical separation by the selection of appropriate reaction conditions, such as reaction duration and reagent pressure.

4. Summary

With all of the alkenes studied, the dehydrogenation (and cracking) activity of Cf^+ was minimal; only with cyclohexadiene was a very minor amount of the dehyrogenation product, Cf^+–benzene, detected. Direct comparison between the results for Cm^+ and Cf^+ indicated a relative C–H activation efficiency (k/k_{ADO}) for Cf^+ of $\ll$1% that of Cm^+. The results for Cf^+ are consistent with a C–H activation mechanism requiring insertion of the metal center into a C–H bond, C–Cf^+–H, and the estimated large promotion energy, $>$200 kJ mol^{-1}, required to achieve an electronic configuration of Cf^+ with two non-5*f* valence electrons at the metal center. It is apparent that the 5*f* electrons of Cf^+ are insufficiently delocalized to participate directly in organometallic σ-bond formation. With cyclooctatetraene, the Cf^+–COT condensation adduct was produced, suggesting the feasibility of preparing condensed phase compounds comprised of a trivalent Cf metal site π-bonded to COT.

Reactions of the metal ions with butryonitrile produced the adducts, M^+–butryonitrile and MO^+–butryonitrile for M = Cf, Pr, and Tm; only for Pr^+ was a minor degree of dehydrogenation induced, reflecting the relative ease of C–H activation by this ion. The CfO^+–butyronitrile complex was the only species where bonding of CfO^+ was manifested; attempts to oxidize Cf^+ to CfO^+ with N_2O, and thereby obtain larger amounts of CfO^+ reactant, were unsuccessful. Reflecting the ineffective insertion of Cf^+ into N–H and C–H bonds, the primary product with butylamine was the adduct, Cf^+–$C_4H_{11}N$. A remarkable result was the apparent formation with Cf^+ and Tm^+ of the 3H-loss product, M^+–C_4H_8N; the loss of H_2 + H from butylamine should be quite endothermic and this reaction channel is postulated to result in complexes comprising strong metal-nitrogen σ-type bonds, M^+–N=CH–C_3H_7.

Ethanedithiol was studied here primarily because intriguing species had resulted from its reaction with lighter actinide ions. The primary species found here were the divalent hydrosulfide, $Cf(SH)^+$, and the trivalent monosulfide, CfS^+; disulfide (presumably persulfide complex), CfS_2^+; and the bis-hydrosulfide, $Cf(SH)_2^+$. These novel species offer a distinctive comparison with the corresponding oxide and hydroxide species; hydrosulfide synthesis enables particularly intriguing chemistry.

Reactions with ethers, particularly dimethyl ether, were consistent with the relatively low reactivity, presumably C–O activation in this instance, of Cf^+. In addition to a detectable Cf^+–ether adduct, a minor amount of californium monomethoxide, Cf^+–OCH_3, was also produced. In distinct contrast, the yield of Cm^+–OCH_3 was nearly 10^3 times that of Cf^+–OCH_3, and a significant amount of trivalent Cm^+–$(OCH_3)_2$ [and/or CmO^+–(CH_3OCH_3)] was additionally produced. No trivalent Cf^+–$(OCH_3)_2$ was detected and it is predicted that the formation of volatile californium alkoxides should require relatively rigorous oxidation conditions.

Fluorine atom abstraction was investigated using hexafluoropropene and perfluorophenanthrene as reagents. Based on the IE[M^+] and IE[M^{2+}] of the studied *f* elements, it is expected that under conditions of sufficiently long reaction times and/or high reagent pressures, MF_2^+ should be the ultimate product in all cases. However, relatively small differences in IEs were manifested as large discrepancies in product yields under LAPRD conditions. Furthermore, substantial differences were obtained depending on the reagent pressure, which were higher for hexafluoropropene than perfluorophenanthrene. With regard to the specific chemistry of Cf, its propensity to exist in a divalent state was clearly manifested by the minor yield of CfF_2^+ compared with that of CmF_2^+ ($<$10% relative abundance) with both reagents. More controlled reaction conditions could result in an even

greater differentiation between Cf and Cm (as well as other actinides). A potential application of this effect is for the mass-spectrometric analysis of isobaric ^{249}Bk and its ^{249}Cf daughter. The former is expected to oxidize more readily to the trivalent state (IE[Bk^{2+}] = 2150 kJ mol^{-1} [48]), and may even produce tetravalent species, such as $BkOF^{+}$ or BkF_3^{+}, under suitable reaction conditions (IE[Bk^{3+}] = 3430 kJ mol^{-1} [48]).

Acknowledgements

Research sponsored by the Division of Chemical Sciences, Geosciences, and Biosciences, Office of Basic Energy Sciences, U.S. Department of Energy, under contract no. DE-AC05-00OR22725 with Oak Ridge National Laboratory, managed and operated by UT-Battelle, LLC. The ^{249}Cf used in this study was supplied by the Division of Chemical Sciences, Office of Science, U.S. Department of Energy, through the transplutonium element production facilities located at the Oak Ridge National Laboratory.

References

[1] Organometallic Ion Chemistry; B.S. Freiser (Ed.), Kluwer, Dordrecht, 1996.
[2] K. Eller, H. Schwarz, Chem. Rev. 91 (1991) 1121.
[3] K.J. Fisher, I.G. Dance, G.D. Willett, Rapid Commun. Mass Spectrom. 10 (1996) 106.
[4] J.J. Katz, L.R. Morss, G.T. Seaborg, in The Chemistry of the Actinide Elements, 2nd ed., J.J. Katz, G.T. Seaborg, L.R. Morss (Eds.), Chapman and Hall, New York, 1986, Vol. 2, pp. 1121–1195.
[5] The Chemistry of the Actinide Elements, J.J. Katz, G.T. Seaborg, L.R. Morss (Eds.), 2nd ed., Chapman and Hall, New York, 1986, Vol. 2.
[6] G.K. Liu, S.T. Li, J.V. Beitz, M. Abraham, J. Alloys Compd. 271 (1998) 872.
[7] J.K. Gibson, J. Phys. Chem. 100 (1996) 15688.
[8] B.S. Freiser, Acc. Chem. Res. 27 (1994) 353.
[9] J.B. Schilling, J.L. Beauchamp, J. Am. Chem. Soc. 110 (1988) 15.
[10] H.H. Cornehl, C. Heinemann, D. Schroder, H. Schwarz, Organometallics 14 (1995) 992.
[11] W.W. Yin, A.G. Marshall, J. Marcalo, A. Pires de Matos, J. Am. Chem. Soc. 116 (1994) 8666.
[12] D.H. Russell, J.V.B. Oriedo, T. Solouki, in Organometallic Ion Chemistry, B.S. Freiser (Ed.), Kluwer, Dordrecht, 1996, pp. 197–228.
[13] L.S. Sunderlin, P.B. Armentrout, J. Am. Chem. Soc. 111 (1989) 3845.
[14] F.A. Cotton, G. Wilkinson, Advanced Inorganic Chemistry, 5th ed., Wiley, New York, 1988, pp. 955.
[15] F. Weigel, J.J. Katz, G.T. Seaborg , in The Chemistry of the Actinide Elements, 2nd ed., J.J. Katz, G.T. Seaborg, L.R. Morss (Eds.), Chapman and Hall, New York, 1986, Vol. 1, pp. 499–886.
[16] S. Heathman, R.G. Haire, J. Alloys Compd. 271 (1998) 342.
[17] G.Y. Hong, F. Schautz, M. Dolg, J. Am. Chem. Soc. 121 (1999) 1502.
[18] P.B. Armentrout, R.V. Hodges, J.L. Beauchamp, J. Chem. Phys. 66 (1977) 4683.
[19] Z. Liang, A.G. Marshall, A. Pires de Matos, J.C. Spirlet, in Transuranium Elements: A Half Century," L.R. Morss, J. Fuger (Ed.), American Chemical Society, Washington, DC, 1992, pp. 247–250.
[20] C. Heinemann, H.H. Cornehl, H. Schwarz, J. Organomet. Chem. 501 (1995) 201.
[21] J. Marcalo, J.P. Leal, A. Pires de Matos, Int. J. Mass Spectrom. Ion Processes 157/158 (1996) 265.
[22] J. Marcalo, J.P. Leal, A. Pires de Matos, A.G. Marshall, Organometallics 16 (1997) 4581.
[23] J.K. Gibson, Organometallics 16 (1997) 4214.
[24] J.K. Gibson, J. Am. Chem. Soc. 120 (1998) 2633.
[25] J.K. Gibson, Organometallics 17 (1998) 2583.
[26] J.K. Gibson, R.G. Haire, J. Phys. Chem. A 102 (1998) 10746.
[27] W.C. Martin, R. Zalubas, L. Hagan, Atomic Energy Levels—The Rare Earth Elements, U.S. Dept. of Commerce, National Bureau of Standards (NIST), Washington, DC, 1978.
[28] M.S. Fred, J. Blaise, in The Chemistry of the Actinide Elements, 2nd ed., J.J. Katz, G.T. Seaborg, L.R. Morss, (Eds.), Chapman and Hall, New York, 1986, Vol. 2, pp. 1196–1277.
[29] L. Brewer, J. Opt. Soc. Am. 61 (1971) 1666.
[30] K. Eller, in Organometallic Ion Chemistry, B.S. Freiser, (Ed.), Kluwer, Dordrecht, 1996, pp. 123–155.
[31] J.K. Gibson, Inorg. Chem. 38 (1999) 165.
[32] J.K. Gibson, J. Mass Spectrom. 34 (1999) 1166.
[33] (a) K.K. Irikura, E.H. Fowles, J.L. Beauchamp, Anal. Chem. 66 (1994) 3447; (b) J.K. Gibson, J. Fluorine Chem. 78 (1996) 65.
[34] J.K. Gibson, J. Alloys Compd. 290 (1999) 52.
[35] S.G. Lias, J.E. Bartmess, J.F. Liebman, J.L. Holmes, R.D. Levin, W.G. Mallard, Gas-Phase Ion and Neutral Thermochemistry, American Chemical Society, Washington, DC, 1988.
[36] R.G. Haire, J. Alloys Compd. 213/214 (1994) 185.
[37] M.S. Chandrasekharaiah, K.A. Gingerich, in Handbook on the Chemistry and Physics of Rare Earths, K.A. Gschneidner Jr., L. Eyring (Eds.), North-Holland, Amsterdam, 1989, Vol. 12, Chap. 86, pp. 409–431.
[38] (a) P.B. Armentrout, L.F. Halle, J.L. Beauchamp, J. Chem. Phys. 76 (1982) 2449; (b) D. Ritter, J.C. Weisshaar, J. Phys. Chem. 93 (1989) 1576.

[39] H.H. Cornehl, R. Wesendrup, M. Diefenbach, H. Schwarz, Chem. Eur. J. 3 (1997) 1083.
[40] P.G. Laubereau, J.H. Burns, Inorg. Chem. 9 (1970) 1091.
[41] R.G. Haire, in The Chemistry of the Actinide Elements, 2nd ed., J.J. Katz, G.T. Seaborg, L.R. Morss, (Eds.), Chapman and Hall, New York, 1986, Vol. 2, pp. 11025–1070.
[42] T.J. Marks, A. Streitweiser Jr., in The Chemistry of the Actinide Elements, 2nd ed., J.J. Katz, G.T. Seaborg, L.R. Morss, (Eds.), Chapman and Hall, New York, 1986, Vol. 2, pp. 1547–1587.
[43] T.J. Marks, in The Chemistry of the Actinide Elements, 2nd ed., J.J. Katz, G.T. Seaborg, L.R. Morss, (Eds.), Chapman and Hall, New York, 1986, Vol. 2, pp. 1588–1628.
[44] A. Streitweiser Jr., U. Muller-Westerhoff, J. Am. Chem. Soc. 90 (1968) 7364.
[45] R.D. Shannon, Acta Cryst. A 32 (1976) 751.
[46] S. Barsch, I. Kretzschmar, D. Schroder, H. Schwarz, P.B. Armentrout, J. Phys. Chem. A 103 (1999) 5925.
[47] NIST Chemistry WebBook, NIST Standard Reference Database Number 69, W.G. Mallard, P.J. Linstrom, (Eds.), National Institute of Standards and Technology, Gaithersburg, MD, 1998 (http://webbook.nist.gov).
[48] L.R. Morss, in The Chemistry of the Actinide Elements, 2nd ed., J.J. Katz, G.T. Seaborg, L.R. Morss (Eds.), Chapman and Hall New York, 1986 Vol. 2, pp. 1278–1360.
[49] M. Sakanoue, R. Amano, in Transplutonium 1975, W. Muller, R. Lindner (Eds.), North-Holland, Amsterdam, 1976, pp. 123–129.
[50] H.H. Cornehl, G. Hornung, H. Schwarz, J. Am. Chem. Soc. 118 (1996) 9960.